Porous beta tricalcium phosphate scaffolds used as a BMP-2 delivery system for bone tissue engineering

Jérôme Sohier,[1] Guy Daculsi,[1] Sophie Sourice,[1] Klaas de Groot,[2] Pierre Layrolle[1]
[1]*Inserm, U791, Laboratory for Osteo-Articular and Dental Tissue Engineering, Faculty of Dental Surgery, University of Nantes, BP 84215, 44042 Nantes, France*
[2]*Department of Tissue Regeneration, University of Twente, Institute for BioMedical Technology, P.O. Box 217, Enschede 7500 AE, The Netherlands*

Received 3 July 2008; revised 16 January 2009; accepted 27 January 2009
Published online 19 March 2009 in Wiley InterScience (www.interscience.wiley.com). DOI: 10.1002/jbm.a.32467

Abstract: Macroporous beta tricalcium phosphate (β-TCP) scaffolds were evaluated as potential carriers and delivery systems for bone morphogenetic protein-2 (BMP-2). Chemical etching was performed to increase the available surface and thus the protein loading. X-ray diffraction and infrared spectrocopy analyses confirmed the preparation of pure β-TCP scaffolds. Scanning electron microscopy revealed interconnected porosity (64%) and a microporous surface after chemical etching. Scaffolds loaded with 30 and 15 μg of BMP-2 were implanted respectively into the back muscles and into femoral defects (condyle and diaphysis) of rabbits for 4 weeks. Histological observations confirmed the activity of the BMP-2 released from the scaffolds. Intramuscularly, bone was formed within the BMP-2-loaded scaffold pores. In the bone defects, the effect of released BMP-2 was similarly noticeable, as evaluated by histomorphometry. The incorporation of BMP-2 resulted in an amount of newly formed bone that was 1.3 times higher than with unloaded scaffolds. The implant site, however, did not have an effect on bone formation as no statistical differences were measured between cortical (diaphysis) and trabecular (condyle) defects. These results indicate the suitability of chemically etched β-TCP scaffolds as BMP-2 carriers, in the context of bone regeneration. © 2009 Wiley Periodicals, Inc. J Biomed Mater Res 92A: 1105–1114, 2010

Key words: tricalcium phosphate; ceramic; bone morphogenetic protein-2; osteogenesis

INTRODUCTION

Calcium phosphate (CaP) ceramics are widely used as bone substitutes in orthopedic, maxillofacial, or spine surgery.[1–4] These synthetic bone fillers are generally composed of beta-tricalcium phosphate (β-TCP), hydroxyapatite (HA), or biphasic calcium phosphates (BCP) and manufactured in various forms, from macroporous blocks to granules, powders, or coatings.[5,6] Several studies have shown that CaP ceramics are bioactive and osteoconductive. After implantation into bone defects, CaP ceramics interact with body fluids leading to partial dissolution and precipitation of biological carbonated apatite on to their surface.[7,8] The apatite layer formed *in vivo* contains various endogenous proteins and is colonized by osteoblastic cells producing the bone extracellular matrix.[9] As a result of this bioactivity, CaP ceramics guide bone healing on their surface by means of osteoconduction.[5] The solubility of CaP ceramics is mainly related to their chemical composition and β-TCP presents a greater degradation rate than HA. Accordingly, β-TCP induces a greater amount of precipitated apatite.[10]

Although these synthetic fillers support the bone-healing process, they generally lack osteoinductivity for the regeneration of bone tissue over large defects. Nevertheless, it has recently been shown that microporous calcium phosphate bioceramics can induce ectopic bone formation after 6–12 weeks of implantation into the muscles of large animals, without the addition of osteogenic cells or bone growth factors.[11–16] It has been shown that microporosity obtained by relatively low temperature sintering is a prerequisite for inducing ectopic bone formation.[17] Several authors have hypothesized that microporous CaP ceramics may concentrate endogenous growth factors such as bone morphogenetic proteins (BMPs).[18–21] BMPs have a high affinity with calcium phosphates. Nevertheless, the possible concentration of endogenous cytokines by calcium phosphates has not been clearly demonstrated. Many studies have investigated the osteogenic properties of BMPs/calcium phosphate combinations. The most studied system is BMP-2-loaded in

Correspondence to: P. Layrolle; e-mail: pierre.layrolle@nantes.inserm.fr

calcium phosphate cements (CPC).[22–24] Nevertheless, CPC do not have sufficient porosity to allow bone ingrowth. Porous calcium phosphate ceramics have also been used as carriers of BMPs[25,26] and have been shown to induce ectopic bone formation. It is well known that BMPs differentiate mesenchymal stem cells into osteoblasts.[27,28] Since the pioneering work of Urist using demineralized bone matrix, recombinant BMPs have been genetically produced and associated with natural or synthetic carriers and induced ectopic bone formation *in vivo*. For instance, BMP-loaded collagen sponges can differentiate circulating stem cells into first chondrocytes and then osteoblasts to produce mineralized bone tissue within few weeks of implantation under the skin of rodents.[29–31] The combination of BMP and collagen sponges has even been used in clinical situations for bone reconstruction purposes.[32,33] However, collagen carriers are rapidly degraded *in vivo* leading mainly to a burst release of BMP into the body fluids. An appropriate carrier for BMPs as well as a suitable delivery profile are therefore conditions for successful osteoinductive fillers. In addition, the combination of micro- and macroporous calcium phosphate ceramics with BMP-2 may potentiate bone formation by combining osteoinductive and osteconductive properties.

The purpose of this study was to investigate the osteogenic properties of BMP-2 combined with β-TCP scaffolds in both intramuscular and bone defects in rabbits. This model was selected according to our large experience in this type of defect for evaluation of osteogenic property of calcium phosphate bioceramics. So far, orthotopic calvaria models were used for BMP evaluation and for tissue induction and morphogenesis by osteoinductive biomimetic matrices.[34,35] In the first step, the capacity of β-TCP scaffolds to retain proteins was evaluated *in vitro* in conjunction with a chemical treatment of the scaffold to increase the available surface. BMP-2 being an expensive protein, its association with scaffolds should be as effective as possible to prevent loss. β-TCP was preferred over HA or BCP to provide an important apatite precipitation. Then BMP-2-loaded scaffolds were evaluated *in vivo* intramuscularly and in bone defects in rabbits with regard to their bone-forming capacity. Defects in trabecular and cortical bone locations were used to elucidate the influence of surrounding bone type on bone formation.

MATERIALS AND METHODS

Preparation of the macro/microporous β-TCP ceramics

The porous β-TCP ceramics were produced using the dual-phase mixing method (IsoTis, Bilthoven, The Netherlands).[36,37] In this process, a water-based β-TCP slurry was mixed with poly-methyl methacrylate (PMMA) resin and MMA monomer. The commercial β-TCP powder (Fluka Chemie BV) was first calcinated at 1000°C with heating and a cooling rate of 100°C/h with no holding stage. To prepare a stable slurry, the calcinated β-TCP (67.3 wt %) was thoroughly mixed with demineralized water (28.6 wt %), ammonia solution (25 vol %, Merck), defloculant (Dolapix CE64, Aschimmer, and Schwarz, Germany) and binder (sodium carboxymethyl cellulose, 1 wt % CMC, Pomosin BV, Bunschoten, The Netherlands). This ceramic slurry was then mixed with PMMA powder (Dentalbiolux International, Belgium) containing 1% benzoyl peroxide (BPO, Merck) which served as a radical polymerization initiator. To obtain porosities higher than 50% for the final ceramic, small amounts of naphthalene (10 wt %, Aldrich) particles were also added to the mixture. Prior to use, the naphtalene powder was sieved between 600 and 1000 μm to achieve the final pore size in the ceramic. MMA liquid (Merck) containing 2% *N*,*N*-demethyl*p*-toluidine (DMPT; Aldrich, Milwaukee, WI), acting as an accelerator for polymerization, was added to the mixture with vigorous hand mixing. The volume ratio of β-TCP slurry to MMA/PMMA mixture was 1:1. The mixture polymerized, forming a semi-solid mass in which the β-TCP slurry was embedded. The vigorous hand mixing led to an interpenetrated network of the two immiscible organic (PMMA) and mineral (β-TCP) phases. The polymerized blocks were dried at 50°C overnight in air. Finally, the blocks were placed in a furnace (Nabertherm; Lilienthol, Germany) for pyrolysis of the organics and direct sintering of the β-TCP ceramic. According to thermal gravimetric analysis (TGA, PerkinElmer, Norwalk, CT) all the organics were completely burned out in air at ~440°C.[36] To prevent blistering and cracking of the β-TCP green bodies, a slow heating rate of 1°C/min was used up to 500°C. The β-TCP green bodies were subsequently heated at 1150°C with a rate of 100°C/h, held at this temperature for 8 h to complete sintering, and allowed to cool down at room temperature at the same rate. The macroporous β-TCP ceramic blocks were cut into 10 × 10 × 4 mm shaped implants using a diamond saw and machined into cylinders Ø 2.7 × 5 mm with a lathe. To create microporosity, the β-TCP ceramics were dipped into citric acid solution (1%) for 1 min, then thoroughly rinsed in demineralized water, ultrasonically cleaned in ethanol and acetone for 10 min and finally dried in air for a few hours. The shaped β-TCP implants were individually packaged and sterilized by gamma irradiation at 25 kGy (Gammaster BV, The Netherlands).

Characterization of the macro/microporous β-TCP ceramics

Phase purity of β-TCP ceramics was determined by using both X-ray diffraction (XRD, Rigaku Miniflex, Tokyo, Japan) and Fourier Transform Infrared spectroscopy (FTIR, Perkin-Elmer Spectrum 1000). Total porosity of macro/microporous β-TCP ceramics was determined from relative density by precisely measuring the weight and dimensions of the cylindrical samples. The theoritical density of 3.07 g/cm^3 for β-TCP was used in the calculation of total

porosity. Macroporous structure was observed with a stereo-optic microscope (Nikon SMZ-10A) equipped with a CCD camera (Sony Progressive 3CCD color video camera). To measure macropore size, a piece of β-TCP was sawed with a diamond saw and then the cross-section was polished with a series of SiC sand papers. After cleaning in an ultrasound water bath and drying, the cross-section was observed with environmental scanning electronic microscopy (ESEM-FEG XL 30; Philips; Eindhoven, The Netherlands) at low magnification. The macropore size was averaged from at least 30 measurements. The microstructures of prepared and acid-etched β-TCP ceramics were compared under ESEM at magnification 2000×.

Protein loading capacity of the macro/microporous β-TCP ceramics

β-TCP ceramics with a size of 10 × 10 × 4 mm and a weight of 0.44 g were used to study their capacity to be loaded with proteins. First, the quantity of water taken by the macro/microporous β-TCP ceramic was measured by weighing eight blocks before and after soaking in demineralized water for 1 h. Second, a model protein, bovine serum albumin (BSA, Sigma-Aldrich Chemie BV, Zwijndrecht) was used for testing protein loading capacity on to β-TCP acid-etched and non-etched ceramics. The samples were placed in 12-well plates for cell culture (Nunc, Roskilde, Denmark). Each well was filled with 1750 μL of BSA solution and immediately put on a shaking plate at 120 rpm. The BSA concentration in the wells was 100 μg/mL and experiments were performed in triplicate. After incubation for 1, 1.5, and 2 h, 100 μL of excess BSA solution were pipetted and put into ELISA flat bottom 96-well plates (Maxisorp; Nunc) for 2 h at 37°C. The plates were then rinsed three times with TBS/TWEEN and blocked with 200 μL of 1% wt/vol gelatin in TBS for 30 min at 37°C. After removing the blocking solution, 100 μL of mouse anti-BSA immunoglobulin (Sigma-Aldrich) diluted in gelatin/TBS/TWEEN was added to each well and stored at 37°C for 1.5 h. The plates were again washed three times with TBS/TWEEN. Then, 100 μL of the second antibody (rabbit anti-mouse immunoglobulin conjugated with alkaline phosphatase) in gelatin/TBS/TWEEN were added and incubated at 37°C for 1.5 h. After washing three times with TBS/TWEEN, enzymatic activity was revealed with a fluorescent substrate solution composed of disodium p-nitrophenylphosphate (Sigma-Aldrich) and reading at 405 nm by using a multi-plate reader (El 312e, BioTek instruments). Optical density results were directly converted into concentrations using BSA standards.

In vivo study

Sample preparation

Recombinant Human Bone Morphogenetic Protein-2 (rhBMP-2) was provided by Genetics Institute Corp. Cambridge, USA. For intramuscular implantation, a stock solution was prepared by dissolving 146 μg of rhBMP-2 per mL of sterile water. Each cubic plate of macro/microporous β-TCP ceramic was loaded with 200 μL of the rhBMP-2 solution. The total amount of rhBMP-2 was therefore ~30 μg rhBMP-2 per intramuscular implant. For intrafemoral implantation, a stock solution containing 1122 μg of rhBMP-2 per mL of sterile water was prepared. The macro/microporous β-TCP ceramic cylinders were placed in a 96-well plate (Nunc). Each cylinder received 15 μL of this rhBMP-2 solution giving a total amount of 15 μg rhBMP-2 per intrafemoral implant. Both types of macro/microporous β-TCP ceramic implant loaded with rhBMP-2 were left for 2 h under aseptic conditions. The amount of BMP-2 used for intrafemoral implants was twice higher than the one used for intramuscular implants to compensate for the higher volume of the latter, while remaining in reasonable quantities of growth factor.

Animals

This study has been approved by the Local Ethical Committee for Animal Care (Utrecht Medical University, The Netherlands). Sixteen female New Zealand White (NZW) rabbits, about 6 months old, weighing approximately 3.5–4.5 kg, were purchased from a local breeder. The animals were housed in individual cages measuring 75 × 47 × 40 cm at the Laboratory for Animal Experimentation (GDL, Utrecht). The rabbits were fed daily with granular food (35 g/kg body weight) and water *ad libidum*. The national guidelines for the care and use of laboratory animals were strictly observed. The materials were implanted in female New Zealand White rabbits for a follow-up time of 4 weeks.

Surgical procedure

Methadon and Acepromazine were injected intramuscularly as premedication. The rabbits were anesthetized by intravenous injection of Etomidat (0.3 mg/kg body weight) and an endotracheal tube was inserted to prevent aspiration. The surgical procedure was performed under general inhalation anesthesia by a mixture of nitrous oxide and oxygen (1:1) and 1% Halothane. The implantation areas (lumbar back muscles and femurs) were shaved and disinfected with iodine (2% in alcohol 50%).

For intramuscular implantation, two skin and muscle incisions of ~2 cm were made at a distance of 2 cm in the lumbar region on the right side of the spine. Two β-TCP ceramic cubic plates (one with and one without rhBMP-2) were inserted into the back muscle. The muscles and skin were closed separately with 3–0 Vicryl sutures. The total number of samples was 16 loaded with BMP-2 and 16 unloaded, implanted in 16 rabbits.

For intrafemoral implantation, a 4-cm incision was made in the skin, muscle fascia, and femoral periosteum. Two defect sites were created in the right femoral condyle and in the right femoral diaphysis using a 2.7 mm diameter dental drill cooled with saline solution. Two macro/microporous β-TCP ceramic cylinders (one with and one without rhBMP-2) were press-fit implanted randomly into each type of defects (condyle and dyaphisis). Furthermore, 2 condyle and 2 diaphysis defects were left empty as con-

trol. The total number of samples was 14 BMP-2-loaded cylinders in femoral diaphysis (7) and femoral condyle (7), 14 unloaded cylinders in femoral diaphysis (7) and femoral condyle (7), and 2 empty defects in femoral condyle and dyaphisis; distributed in 16 rabbits. After implantation, the periosteum, muscle fascia, subcutis, and skin were closed separately by suturing with 3-0 Vicryl. After surgery, anti-inflammatory medication (Nalbuphine, 1 mg/kg bodyweight) was injected intramuscularly.

Analysis of retrieved implants

The rabbits were sacrificed after 4 weeks by injection of overdoses of Thiopental. After retrieval, the implants and surrounding bone were processed according to standard operating procedures for histology. The blocks were immersed in Karnovsky's fixative (4% formaldehyde, 5% gluteraldehyde), dehydrated in a graded series of ethanol and embedded in methylmethacrylate (MMA). After polymerization, the samples were divided lengthwise through the implant. Half of each implant was sectioned using a modified diamond-saw microtome (Leica, Rijswijk), stained with methylene blue and basic fuchsin and analyzed with light microscopy. The other half was polished and gold sputter-coated using a Cressington 108 auto apparatus prior to analysis with a Leo 1450 VP electronic microscope using Back-Scattered Electron (BSE) mode for histomorphometrical analysis. This makes it possible to segregate bone from the implanted ceramics based on the respective densities of the two substances. In addition to the technical difficulty to reproduce the same level of cross section in all samples, some cylinders were found inside the bone shaft and without direct contact with bone after sectioning. Therefore, some samples were discarded prior histomorphometrical analysis (respectively one, two, and three samples from the groups of BMP-2-loaded cylinders in femoral condyle, BMP-2-loaded cylinders in femoral diaphysis and unloaded cylinders in femoral condyle). The surface of newly formed bone within the ceramic structures was then quantified using image analysis (Quantimet 4, Leica) and a percentage of the surface available within the pores was calculated. Three blinded persons repeated the histomorphometrical measurements. The resulting groups of values obtained from each person were pooled and statistically compared two by two with Student tests at a significance level of 5%. For each pair of conditions compared, the normality of each population was assessed with a chi-squared test and the equality of variance was established with a F-test at a significance level of 5%.

RESULTS

Macroporous β-TCP ceramics were prepared by mixing a slurry with an immiscible polymer phase, followed by sintering at 1150°C. FTIR and XRD analyses indicated pure β-TCP (98% min) without additional phases such as hydroxyapatite (HA) and beta-calcium pyrophosphate β-$Ca_2P_2O_7$ according to the ASTM 1088 standard. Figure 1(A) shows the two types of β-TCP ceramic scaffolds used in this study: cubic plates and cylinders measuring 10 × 10 × 4 mm and Ø 2.7 × 5 mm, respectively. The macro/microporous β-TCP ceramics had an average porosity of 64 ± 1.7%. The β-TCP ceramic implants exhibited interconnected macropores averaging 378 ± 34 μm, as shown in Figure 1(B). The macroporous

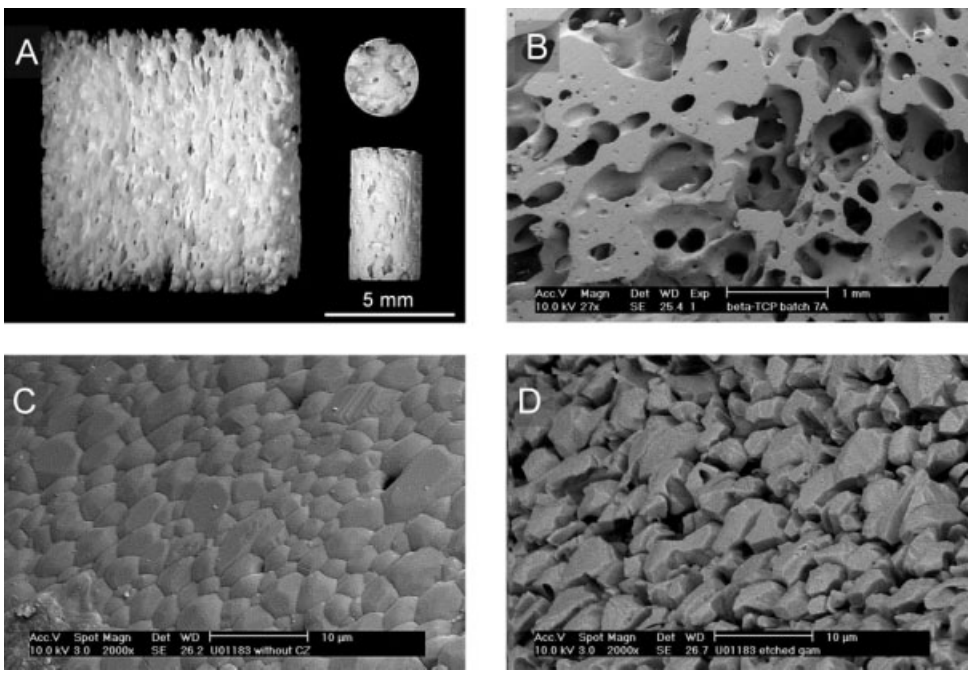

Figure 1. Macroscopic (A and B) and microscopic view of β-TCP porous scaffolds before (C) and after (D) chemical etching.

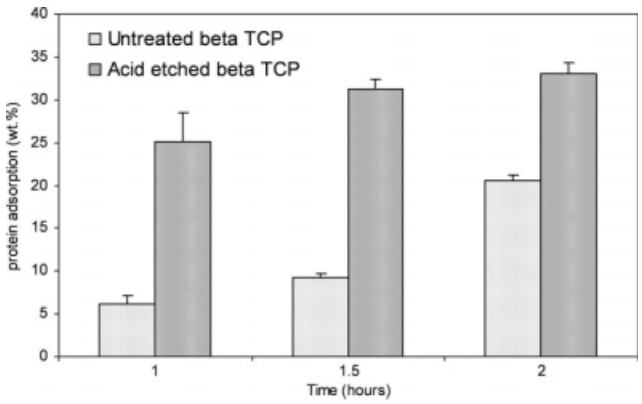

Figure 2. Effect of acid etching of β-TCP scaffolds on BSA adsorption. Initial BSA concentration was 100 μg/mL.

β-TCP ceramics were fully sintered and showed a smooth and dense surface on the inner pores [Fig. 1(C)]. The β-TCP ceramics were briefly etched with citric acid in order to increase surface area and thus protein adsorption. The resulting surface microstructure is shown in Figure 1(D). Grain boundaries appeared selectively etched leading to a rough and microporous surface potentially favorable to protein adsorption. This was evaluated by measuring the capacity of treated and untreated scaffolds to adsorb a model protein (bovine serum albumin, BSA) from a solution when incubated over various times. As can be seen in Figure 2, the chemical etching resulted in an increase of protein uptake by the scaffolds. After 1 h of incubation, 6 weight percent (wt %) of the initial protein amount was taken up by the untreated scaffolds while the etched scaffolds retained four times more BSA (25%). The amount of protein adsorbed increased with longer incubation periods and the increase rate was influenced by the etching treatment. After 2 h of incubation, the untreated scaffolds showed an uptake three times higher than after 1 h (20%) while the amount retained on etched scaffolds increased only slightly (from 25 to 33%). On the basis of the uptake of the model protein on etched and nonetched β-TCP ceramics, an incubation time of 2 h was selected for loading BMP-2 on to etched scaffolds.

Both BMP-2-loaded and unloaded scaffolds were implanted into the muscle and femoral condyles and diaphyses of 16 rabbits for 4 weeks. The rabbits remained healthy and did not show any wound complications after implantation. No inflammatory signs or adverse tissue reaction could be observed at explantation. Figure 3 shows histological sections of β-TCP ceramic plates implanted into the lateral back muscles of rabbits for 4 weeks. The implants that were not treated with a solution of BMP-2 showed no sign of bone formation and the pores were filled

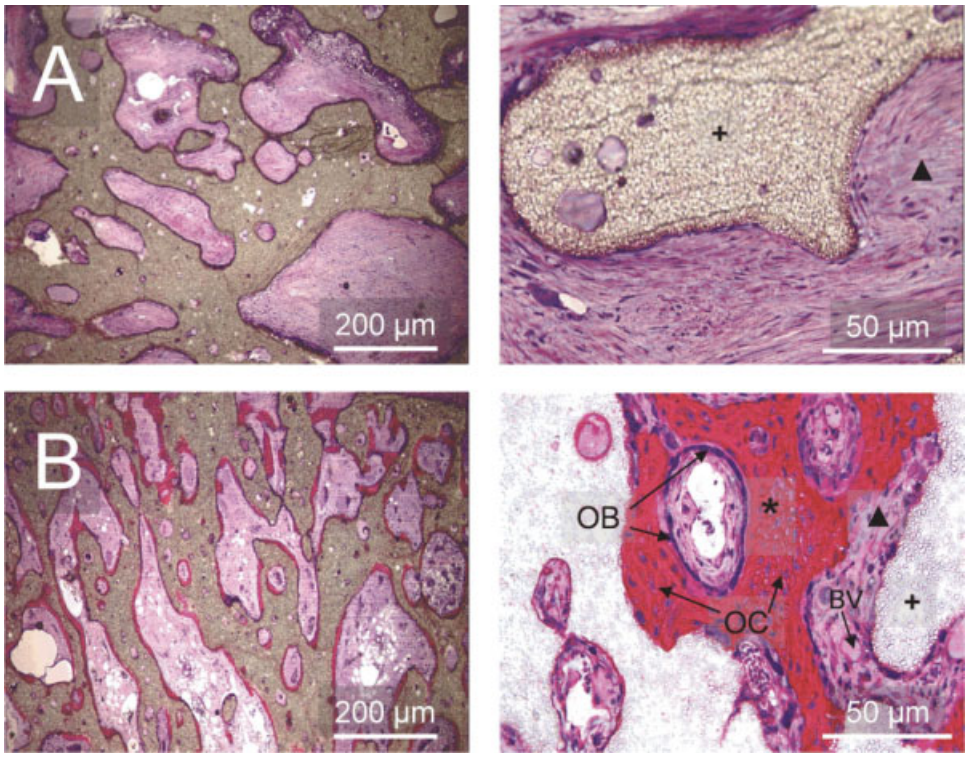

Figure 3. Histological sections of βTCP porous blocks implanted intramuscularly into rabbits for 4 weeks and stained with toluidin blue and basic fuschin. Blocks were left untreated (A) or loaded with BMP2 (B). The newly formed bone appears red (*), the connective tissue is pink (▲) and the ceramic is gray (+). Osteoblasts (OB), osteocytes (OC) and blood vessels (BV) can be observed. [Color figure can be viewed in the online issue, which is available at www.interscience.wiley.com.]

with fibrous tissue. On the contrary, all the blocks treated with BMP-2 showed bone formation, located within the ceramic pores and in direct contact with the ceramic. Osteocytes and osteoblasts were present and the bone appeared mature. Blood vessels could also be seen, underlining the interconnectivity of the scaffolds and accessibility of the inner pores. The β-TCP implants did not show any sign of degradation and no loose particles were observed.

These observations were corroborated using backscattering scanning electron microscopy (BSEM), as presented in Figure 4. The bone formation observed in BMP-2-treated scaffolds was distributed throughout the entire porous block. In many instances, the newly formed bone was not in direct contact with the ceramic surface but was instead distributed within the pores. Histomorphometrical analysis of the bone formation confirmed the presence of bone only in the BMP-2-treated scaffolds. The amount of newly formed bone within the BMP-2-treated β-TCP ceramics was 4.4 ± 3.8%.

With regard to the β-TCP cylinders implanted into the femoral condyles and diaphyses of rabbits for 4 weeks, newly formed bone could be observed macroscopically within the implants after explantation. As shown in Figure 5, histology revealed bone formation within each cylinder, regardless of the investigation conditions (untreated or treated with BMP-2, in femoral condyle or diaphysis). β-TCP implants in trabecular bone (condyle defects) presented a bone ingrowth throughout the complete scaffold, while cylinders implanted into cortical bone (diaphysis defects) showed significant bone formation in the apical part of the cylinders. Accordingly, bone marrow and connective tissues were found in increased abundance in the basal part of the scaffolds, which was directly in contact with the bone marrow. Similar to the β-TCP blocks implanted intramuscularly, no sign of degradation of the cylinders could be found after 4 weeks of implantation. Control empty defects showed a complete bone healing (data not shown).

With regard to the effect of BMP-2 loading, it was difficult to make a visual assessment of any differences in bone formation between samples, independently of the implantation site. A histomorphometrical analysis was performed using BSEM images, the results of which are shown in Figure 6. As a general trend, the adsorption/incorporation of BMP-2 into the β-TCP ceramic structures resulted in greater bone formation as compared with unloaded scaffolds. This increase in bone formation (1.3 times) was independent of the femoral implantation site. BMP-2-loaded and unloaded scaffolds implanted into condyle defects resulted in new bone formation of respectively 33 ± 12 and 26 ± 7%. The same scaffolds implanted in diaphysis defects showed bone formation of 32 ± 9 and 20 ± 8%, respectively. However, this trend was statistically significant only for cylinders implanted into femur diaphyses.

DISCUSSION

With the view to improving the osteogenic potential of β-TCP porous ceramics, their suitability as carriers for recombinant human bone morphogenetic

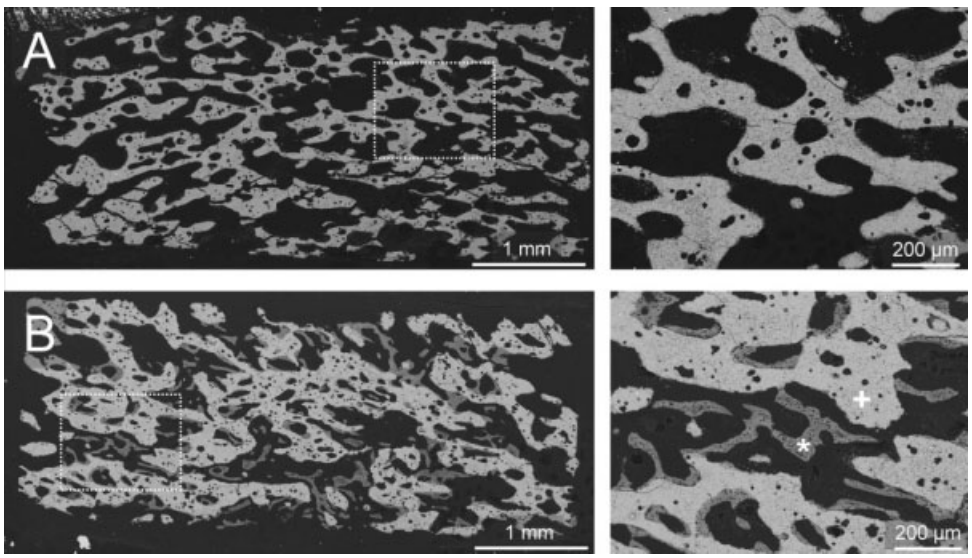

Figure 4. Cross-sections of βTCP porous blocks implanted intramuscularly into rabbits for 4 weeks and observed with back scattering SEM. Blocks were left untreated (A) or loaded with BMP2 (B). Bone appears dark gray (*) while the ceramic is lighter (+).

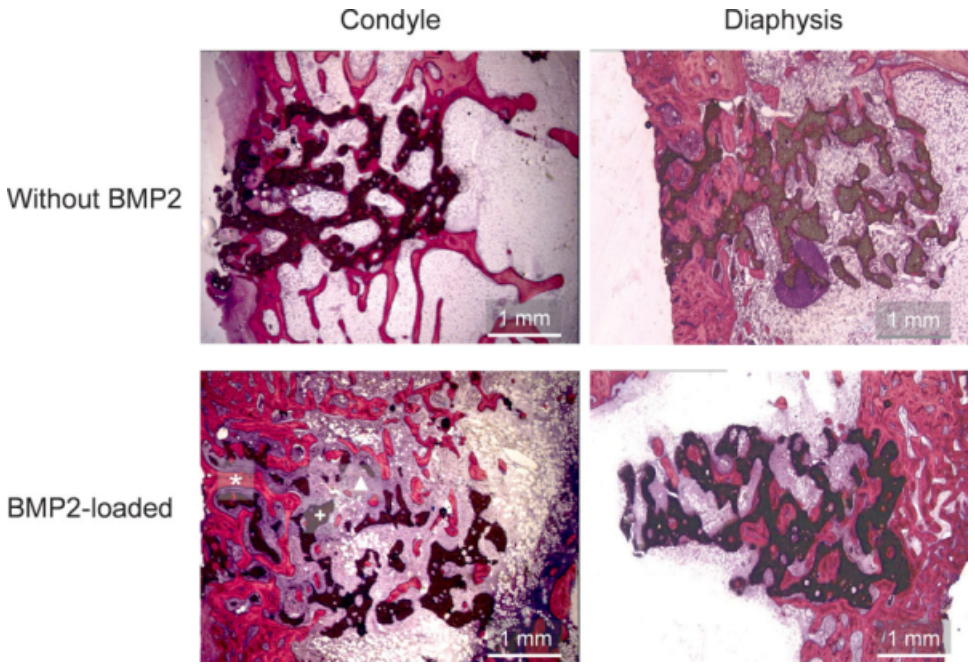

Figure 5. Histological sections of βTCP porous blocks implanted into condyle and diaphysis defects of rabbit femurs for 4 weeks and stained with toluidin blue and basic fuschin. Blocks were loaded with BMP2 or unloaded. The newly formed bone appears red (*), the connective tissue is pink (▲) and the ceramic is gray (+). [Color figure can be viewed in the online issue, which is available at www.interscience.wiley.com.]

protein-2 was here evaluated both intramuscularly and in two different bone defects. Various materials, both organic and inorganic, have been tested as carriers for the local delivery of BMP-2 (such as collagen, poly(α-hydroxy acids, calcium phosphate cement or ceramics).[38–40] However, none of the carrier materials tested so far has proven to be entirely satisfactory. For instance, the relatively fast degradation rate of collagen sponges *in vivo* (~7 days) might result in a too fast elution of the growth factor and a reduced biological effect.[41,42] The BMP-2 delivery profile is known to have an impact on its osteoinductive activity[43] and higher retention rates often yield better results.[44] On the contrary, a single injection of the growth factor *in vivo* is cleared too rapidly to have an effect and induce bone formation. In addition to the retention and local delivery of the growth factor, an optimal material should also be osteoconductive so as to further synergize the BMP-2 effect. This is not the case with poly(α-hydroxy acids), polylactic acid (PLA), or polylactic-*co*-glycolic acid (PLGA) polymers that can provide tailored release rates but are not osteconductive.[45] Calcium phosphate cement (CPC), on the other hand, is bioactive and osteoconductive[46,47] but not porous and does not allow bone ingrowth. Finally, the association of BMP with ceramics was until recently limited to simply depositing the protein on to the surfaces, which mostly results in a fast burst release once in the body. However, a different way of associating growth factors with ceramics, based on the simple adsorption/precipitation of the protein on to the surface, has recently been described.[48–50] It is believed that on contact with a solution containing BMP-2, Ca/P ceramics initiate a dissolution process that ultimately leads to saturation and precipitation of a carbonated apatite on to the surface. During precipitation, the protein is entrapped in the apatite layer by coprecipitation.[51,52] This process, however simple, is limited by the surface readily available for the protein and by the specific affinity of the latter for the surface. These limitations result in inefficient loading of BMP-2 on to the ceramic surface. With these con-

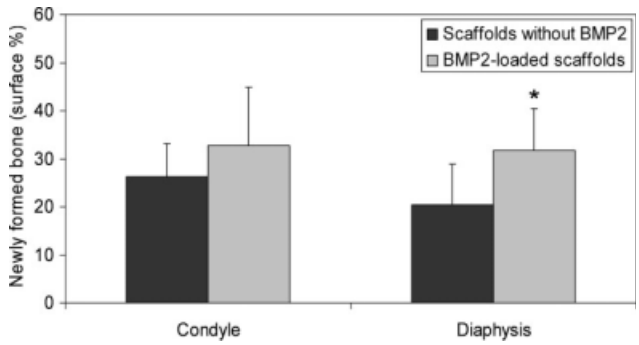

Figure 6. Quantification of newly formed bone within the scaffolds after 4 weeks of implantation. * Denotes a statistically significant difference between samples treated or untreated with BMP2 and implanted into the same site.

siderations in mind, β-TCP ceramics were etched with an acid solution to increase the available surface by the creation of surface microporosity. This approach proved to be effective and resulted in a significant increase in the loading of a model protein (BSA). Interestingly, protein saturation of the ceramics was reached more rapidly for acid-etched than for untreated scaffolds. This suggests that next to surface increase, other mechanisms play a role in the protein uptake improvement seen for etched scaffolds. For instance, the increase of surface roughness results in an increased wettability, which also has an effect on the protein adsorption. It can be as well supposed that the zeta-potential of the scaffold surface is modified by the acid treatment, resulting in higher affinity of the protein.

The successful incorporation of BMP-2 into the etched β-TCP scaffolds was confirmed by intramuscular implantation. The BMP-2-loaded ceramics resulted in osteogenesis within the pores while untreated scaffolds remained filled with connective tissue. These observations indicate that chemically etched β-TCP is an effective carrier of BMP-2. The simple method of association by adsorption/precipitation made it possible to incorporate and release the loaded protein *in vivo* in an active form, thus triggering the formation of bone. The amount of BMP-2 effectively associated to the ceramics after loading was sufficient to induce a tissue response. This is in good agreement with previous work that showed ectopic bone formation after adsorbing different BMP-2 doses on to β-TCP, HA, or BCP ceramics.[26,48,50] However, Alam et al. showed an amount of newly formed bone similar to the one observed here for a BMP-2 dose six times lower (5 μg against 30 μg).[48] Yuan et al. showed a higher level of bone formation for a similar amount of BMP-2 loaded on to cylindrical HA scaffolds. These discrepancies are possibly because of the different animal model used (subcutaneous pockets in rats)[53] and the duration of the implantation (5 weeks), respectively. It is worth noting that the amount of BMP-2 effectively loaded on to ceramic scaffolds is seldom quantified. This renders the comparison of published studies with regard to BMP-2 loading and bone formation very difficult and unreliable. Interestingly, the release was probably not limited to the close vicinity of the ceramic surface as bone was also seen without direct contact with the surface, which indicates the formation of trabeculaes within the pores. It is likely that the BMP-2 release within the pores leads to a concentration increase that allows bone induction. The lack of bone formation within the unloaded scaffolds after 4 weeks of implantation is not surprising and is in good agreement with previously published work.[26] Such a short delay may not be sufficient for the unloaded ceramic matrix to induce bone formation.

Within bone defects, the BMP-2 loading of β-TCP cylinders also resulted in an increase in bone formation, independently of the implantation site. However, this increase in bone in growth was not statistically significant between the two groups when implanted in the condyle defect. In addition, the amount of newly formed bone was similar in the dyaphisis and condyle defects within the BMP-2-loaded group and unloaded group. This is surprising and not in agreement with previous work comparing different implantation sites in rabbits that showed significantly higher osteogenesis in cortical implantation sites than in trabecular and medullar defects.[53,54] It was then argued that a larger contact interface between bone and ceramic in the cortical defects favored bone colonization as compared with trabecular bone (condyle defects). In our case the cylinders implanted in the diaphysis defects were only partly in contact with the cortical bone because of the length of the implant. The other part of the cylinder was in direct contact with the bone marrow, whereas implants in condyle defects were surrounded by trabecular bone. This could explain the absence of difference observed due to better osteoconduction in the condyle defects. Furthermore, trabecular bone (condyle) may contain a higher quantity of stem cells than cortical and medullar bone (diaphysis),[54] which could further enhance bone formation in the condyle defects.

The relatively small effect of the BMP-2 loading is possibly because of the good osteo-integration of the ceramic material and its osteo-conductive properties. In addition to the high level of bone formation observed in BMP-2-unloaded cylinders, the ability of CaP ceramics to repair critical-sized defects alone has been previously reported.[53] The difference between the BMP-2-loaded and unloaded groups was not obvious as bone healing was already significant in defects of 2.75 mm in diameter with TCP cylinders in comparison with empty defects. Furthermore, the animal model is probably of influence as well, considering that empty defects either in condyle or diaphysis sites showed good tissue repair after 4 weeks (data not shown). Although the loading and release of BMP-2 from the ceramic implants is clear, a statistical effect could have been evidenced with defects bigger than 2.75 mm in diameter. However, such defects are difficult in rabbits for anatomical reasons. Previous experiments have effectively shown that rabbit tibial defects with a diameter of 6 mm lead to fractures.[55] Other critical-sized models (distraction ulna or calvaria defects[35]) may show a more significant effect of adding BMP-2 to CaP ceramics. The difficult choice of model can explain the controversial discussions about osteoinduction, particularly in a clinical context which is still a rather difficult goal.[56,57]

CONCLUSION

This study demonstrates the potential of β-TCP scaffolds as a BMP-2 carrier for bone regeneration. The use of chemical etching of the ceramic surface made it possible to increase the protein loading. The resulting effective association of the growth factor with the ceramic scaffold was observed *in vivo* both intramuscularly and in bone defects. The BMP-2 incorporated was sufficient to induce bone within the scaffolds pores. The benefit of BMP-2 was also visible within femoral diaphysis and condyle defects, although not significantly for the latter, suggesting potentialization of the osteoconductives properties of the β-TCP matrices. The animal model and defect size chosen were probably not optimal to measure clearly the beneficial effect of the associated growth factor.

The authors thank the Genetic Institute Corporation for providing the rhBMP-2. Paul van Bergen and Jurren Koerts contributed to the preparation and machining of the macro/microporous β-TCP ceramic implants. Jan Hendriks Boeve is greatly acknowledged for his help in animal experimentation and histology. The authors are grateful to Frédéric Marin, Ph.D. for his expertise in ELISA analysis.

References

1. Hak DJ. The use of osteoconductive bone graft substitutes in orthopaedic trauma. J Am Acad Orthop Surg 2007;15:525–536.
2. Damron TA. Use of 3D beta-tricalcium phosphate (Vitoss) scaffolds in repairing bone defects. Nanomed 2007;2:763–775.
3. Bohner M. Physical and chemical aspects of calcium phosphates used in spinal surgery. Eur Spine J 2001;10(Suppl 2): S114–S121.
4. Passuti N, Daculsi G, Rogez JM, Martin S, Bainvel JV. Macroporous calcium phosphate ceramic performance in human spine fusion. Clin Orthop Relat Res 1989;248:169–176.
5. Jarcho M. Calcium phosphate ceramics as hard tissue prosthetics. Clin Orthop Relat Res 1981;157:259–278.
6. de Groot K. Hydroxylapatite coated implants. J Biomed Mater Res 1989;23:1367–1371.
7. Daculsi G, LeGeros RZ, Mitre D. Crystal dissolution of biological and ceramic apatites. Calcif Tissue Int 1989;45:95–103.
8. Daculsi G, LeGeros RZ, Heughebaert M, Barbieux I. Formation of carbonate-apatite crystals after implantation of calcium phosphate ceramics. Calcif Tissue Int 1990;46:20–27.
9. Barrere F, van Blitterswijk CA, de Groot K. Bone regeneration: Molecular and cellular interactions with calcium phosphate ceramics. Int J Nanomed 2006;1:317–332.
10. G.Daculsi Rzlenklbk. Transformation of biphasic calcium phosphate ceramics *in vivo*: Ultrastructural and physicochemical characterization. J Biomed Mater Res 1989;23:883–894.
11. Ripamonti U. Osteoinduction in porous hydroxyapatite implanted in heterotopic sites of different animal models. Biomaterials 1996;17:31–35.
12. Yang Z, Yuan H, Tong W, Zou P, Chen W, Zhang X. Osteogenesis in extraskeletally implanted porous calcium phosphate ceramics: Variability among different kinds of animals. Biomaterials 1996;17:2131–2137.
13. Yuan H, Zou P, Yang Z, Zhang X, De Bruijn JD, De Groot K. Bone morphogenetic protein and ceramic-induced osteogenesis. J Mater Sci Mater Med 1998;9:717–721.
14. Yuan H, Yang Z, de Bruijn JD, de Groot K, Zhang X. Material-dependent bone induction by calcium phosphate ceramics: A 2.5-year study in dog. Biomaterials 2001;22:2617–2623.
15. Klein C, de Groot K, Chen W, Li Y, Zhang X. Osseous substance formation induced in porous calcium phosphate ceramics in soft tissues. Biomaterials 1994;15:31–34.
16. Yuan H, Van Den Doel M, Li S, Van Blitterswijk CA, De Groot K, De Bruijn JD. A comparison of the osteoinductive potential of two calcium phosphate ceramics implanted intramuscularly in goats. J Mater Sci Mater Med 2002;13:1271–1275.
17. Habibovic P, Yuan H, van der Valk CM, Meijer G, van Blitterswijk CA, de Groot K. 3D microenvironment as essential element for osteoinduction by biomaterials. Biomaterials 2005;26:3565–3575.
18. Ripamonti U. Bone induction in nonhuman primates. An experimental study on the baboon. Clin Orthop Relat Res 1991; 269:284–294.
19. Ripamonti U. Osteoinduction in porous hydroxyapatite implanted in heterotopic sites of different animal models. Biomaterials 1996;17:31–35.
20. Le Nihouannen D, Daculsi G, Saffarzadeh A, Gauthier O, Delplace S, Pilet P, Layrolle P. Ectopic bone formation by microporous calcium phosphate ceramic particles in sheep muscles. Bone 2005;36:1086–1093.
21. De Groot J. Carriers that concentrate native bone morphogenetic protein in vivo. Tissue Eng 1998;4:337–341.
22. Seeherman HJ, Azari K, Bidic S, Rogers L, Li XJ, Hollinger JO, Wozney JM. rhBMP-2 delivered in a calcium phosphate cement accelerates bridging of critical-sized defects in rabbit radii. J Bone Joint Surg Am 2006;88:1553–1565.
23. Miranda DA, Blumenthal NM, Sorensen RG, Wozney JM, Wikesjo UM. Evaluation of recombinant human bone morphogenetic protein-2 on the repair of alveolar ridge defects in baboons. J Periodontol 2005;76:210–220.
24. Seeherman HJ, Bouxsein M, Kim H, Li R, Li XJ, Aiolova M, Wozney JM. Recombinant human bone morphogenetic protein-2 delivered in an injectable calcium phosphate paste accelerates osteotomy-site healing in a nonhuman primate model. J Bone Joint Surg Am A 2004;86:1961–1972.
25. Laffargue P, Hildebrand HF, Rtaimate M, Frayssinet P, Amoureux JP, Marchandise X. Evaluation of human recombinant bone morphogenetic protein-2-loaded tricalcium phosphate implants in rabbits' bone defects. Bone 1999;25(2 Suppl): 55S–58S.
26. Yuan H, De Bruijn JD, Zhang X, Van Blitterswijk CA, De Groot K. Use of an osteoinductive biomaterial as a bone morphogenetic protein carrier. J Mater Sci Mater Med 2001;12:761–766.
27. Sampath TK, Reddi AH. Dissociative extraction and reconstitution of extracellular matrix components involved in local bone differentiation. Proc Natl Acad Sci USA 1981;78:7599–7603.
28. Urist MR, Strates BS. Bone morphogenetic protein. J Dent Res 1971;50:1392–1406.
29. Liu Y, Hunziker EB, Valk CVD, Groot KD. Biomimetic coatings vs. collagen sponges as a carrier for BMP-2: A comparison of the osteogenic responses triggered in vivo using an ectopic rat model. Bioceramics 2003;16:619–622.
30. Otsuru S, Tamai K, Yamazaki T, Yoshikawa H, Kaneda Y. Circulating bone marrow-derived osteoblast progenitor cells are recruited to the bone-forming site by the CXCR4/stromal cell-derived factor-1 pathway. Stem Cells 2008;26:223–234.
31. Wang EA, Rosen V, D'Alessandro JS, Bauduy M, Cordes P, Harada T, Israel DI, Hewick RM, Kerns KM, LaPan P. Recombinant human bone morphogenetic protein induces bone formation. Proc Natl Acad Sci USA 1990;87:2220–2224.

32. Geiger M, Li RH, Friess W. Collagen sponges for bone regeneration with rhBMP-2. Adv Drug Deliv Rev 2003;55:1613–1629.
33. Cook SD. Preclinical and clinical evaluation of osteogenic protein-1 (BMP-7) in bony sites. Orthopedics 1999;22:669–671.
34. Ripamonti U. Soluble osteogenic molecular signals and the induction of bone formation. Biomaterials 2006;27:807–822.
35. Ripamonti U, Ma SS, van den Heever B, Reddi AH. Osteogenin, a bone morphogenetic protein, adsorbed on porous hydroxyapatite substrata, induces rapid bone differentiation in calvarial defects of adult primates. Plast Reconstr Surg 1992;90:382–393.
36. Li S, de Wijn JR, Li J, Layrolle P, de Groot K. Macroporous biphasic calcium phosphate scaffold with high permeability/porosity ratio. Tissue Eng 2003;9:535–548.
37. Li SH, De Wijn JR, Layrolle P, de Groot K. Synthesis of macroporous hydroxyapatite scaffolds for bone tissue engineering. J Biomed Mater Res 2002;61:109–120.
38. Hollinger JO, Leong K. Poly(alpha-hydroxy acids): Carriers for bone morphogenetic proteins. Biomaterials 1996;17:187–194.
39. Kirker-Head CA. Potential applications and delivery strategies for bone morphogenetic proteins. Adv Drug Deliv Rev 2000;43:65–92.
40. Winn SR, Uludag H, Hollinger JO. Sustained release emphasizing recombinant human bone morphogenetic protein-2. Adv Drug Deliv Rev 1998;31:303–318.
41. Yamamoto M, Takahashi Y, Tabata Y. Controlled release by biodegradable hydrogels enhances the ectopic bone formation of bone morphogenetic protein. Biomaterials 2003;24:4375–4383.
42. Urist MR, Lietze A, Dawson E. Beta-tricalcium phosphate delivery system for bone morphogenetic protein. Clin Orthop Relat Res 1984:277–280.
43. Maeda H, Sano A, Fujioka K. Controlled release of rhBMP-2 from collagen minipellet and the relationship between release profile and ectopic bone formation. Int J Pharm 2004;275(1/2):109–122.
44. Uludag H, D'Augusta D, Golden J, Li J, Timony G, Riedel R, Wozney JM. Implantation of recombinant human bone morphogenetic proteins with biomaterial carriers: A correlation between protein pharmacokinetics and osteoinduction in the rat ectopic model. J Biomed Mater Res 2000;50:227–238.
45. Miyamoto S, Takaoka K, Okada T, Yoshikawa H, Hashimoto J, Suzuki S, Ono K. Evaluation of polylactic acid homopolymers as carriers for bone morphogenetic protein. Clin Orthop Relat Res 1992;278:274–285.
46. Lee DD, Tofighi A, Aiolova M, Chakravarthy P, Catalano A, Majahad A, Knaack D. Alpha-BSM: A biomimetic bone substitute and drug delivery vehicle. Clin Orthop Relat Res 1999;367 Suppl:S396–S405.
47. Mickiewicz RA, Mayes AM, Knaack D. Polymer–calcium phosphate cement composites for bone substitutes. J Biomed Mater Res 2002;61:581–592.
48. Alam MI, Asahina I, Ohmamiuda K, Takahashi K, Yokota S, Enomoto S. Evaluation of ceramics composed of different hydroxyapatite to tricalcium phosphate ratios as carriers for rhBMP-2. Biomaterials 2001;22:1643–1651.
49. Long HQ, Li FB, Wang YJ, Liao WM, Wang HX. Osteogenic potential of three kinds of calcium phosphate ceramics as carriers for recombinant human morphogenetic protein-2 in vivo. Zhongguo Xiu Fu Chong Jian Wai Ke Za Zhi 2003;17:180–184.
50. Oda S, Kinoshita A, Higuchi T, Shizuya T, Ishikawa I. Ectopic bone formation by biphasic calcium phosphate (BCP) combined with recombinant human bone morphogenetic protein-2 (rhBMP-2). J Med Dent Sci 1997;44:53–62.
51. Liu Y, de Groot K, Hunziker EB. BMP-2 liberated from biomimetic implant coatings induces and sustains direct ossification in an ectopic rat model. Bone 2005;36:745–757.
52. Liu Y, Hunziker EB, Layrolle P, De Bruijn JD, De Groot K. Bone morphogenetic protein 2 incorporated into biomimetic coatings retains its biological activity. Tissue Eng 2004;10(1/2):101–108.
53. Le Guehennec L, Goyenvalle E, Aguado E, Houchmand-Cuny M, Enkel B, Pilet P, Daculsi G, Layrolle P. Small-animal models for testing macroporous ceramic bone substitutes. J Biomed Mater Res B Appl Biomater 2005;72:69–78.
54. Lu JX, Gallur A, Flautre B, Anselme K, Descamps M, Thierry B, Hardouin P. Comparative study of tissue reactions to calcium phosphate ceramics among cancellous, cortical, and medullar bone sites in rabbits. J Biomed Mater Res 1998;42:357–367.
55. Schmitz JP, Hollinger JO. The critical size defect as an experimental model for craniomandibulofacial nonunions. Clin Orthop Relat Res 1986;205:299–308.
56. Gautschi OP, Frey SP, Zellweger R. Bone morphogenetic proteins in clinical applications. ANZ J Surg 2007;77:626–631.
57. Garrison KR, Donell S, Ryder J, Shemilt I, Mugford M, Harvey I, Song F. Clinical effectiveness and cost-effectiveness of bone morphogenetic proteins in the non-healing of fractures and spinal fusion: A systematic review. Health Technol Assess 2007;11:1–150, iii–iv.